Published OnlineFirst February 20, 2012; DOI:10.1158/1078-0432.CCR-11-1789

Clinical Cancer Research

Protein Kinase CK2 Protects Multiple Myeloma Cells from ER Stress –Induced Apoptosis and from the Cytotoxic Effect of HSP90 Inhibition through Regulation of the Unfolded Protein Response

Sabrina Manni, Alessandra Brancalion, Laura Quotti Tubi, et al.

Clin Cancer Res 2012;18:1888-1900. Published OnlineFirst February 20, 2012.

Published OnlineFirst February 20, 2012; DOI:10.1158/1078-0432.CCR-11-1789

Human Cancer Biology

Clinical Cancer Research

Protein Kinase CK2 Protects Multiple Myeloma Cells from ER Stress–Induced Apoptosis and from the Cytotoxic Effect of HSP90 Inhibition through Regulation of the Unfolded Protein Response

Sabrina Manni[1,2], Alessandra Brancalion[1,2], Laura Quotti Tubi[1,2], Anna Colpo[1,2], Laura Pavan[1,2], Anna Cabrelle[1,2], Elisa Ave[1,2], Fortunato Zaffino[1,2], Giovanni Di Maira[2,3], Maria Ruzzene[2,3], Fausto Adami[1], Renato Zambello[1,2], Maria Rita Pitari[4], Pierfrancesco Tassone[4], Lorenzo A. Pinna[2,3], Carmela Gurrieri[1,2], Gianpietro Semenzato[1,2], and Francesco Piazza[1,2]

Abstract

Purpose: Protein kinase CK2 promotes multiple myeloma cell growth by regulating critical signaling pathways. CK2 also modulates proper HSP90-dependent client protein folding and maturation by phosphorylating its co-chaperone CDC37. Because the endoplasmic reticulum (ER) stress/unfolded protein response (UPR) is central in myeloma pathogenesis, we tested the hypothesis that the CK2/CDC37/HSP90 axis could be involved in UPR in myeloma cells.

Experimental Design: We analyzed CK2 activity upon ER stress, the effects of its inactivation on the UPR pathways and on ER stress–induced apoptosis. The consequences of CK2 plus HSP90 inhibition on myeloma cell growth *in vitro* and *in vivo* and CK2 regulation of HSP90-triggered UPR were determined.

Results: CK2 partly localized to the ER and ER stress triggered its kinase activity. CK2 inhibition reduced the levels of the ER stress sensors IRE1α and BIP/GRP78, increased phosphorylation of PERK and EIF2α, and enhanced ER stress–induced apoptosis. Simultaneous inactivation of CK2 and HSP90 resulted in a synergic anti-myeloma effect (combination index = 0.291) and in much stronger alterations of the UPR pathways as compared with the single inhibition of the two molecules. Cytotoxicity from HSP90 and CK2 targeting was present in a myeloma microenvironment model, on plasma cells from patients with myeloma and in an *in vivo* mouse xenograft model. Mechanistically, CK2 inhibition led to a reduction of IRE1α/HSP90/CDC37 complexes in multiple myeloma cells.

Conclusions: Our results place CK2 as a novel regulator of the ER stress/UPR cascades and HSP90 function in myeloma cells and offer the groundwork to design novel combination treatments for this disease. *Clin Cancer Res; 18(7); 1888–900. ©2012 AACR.*

Introduction

Significant progresses in understanding the pathogenesis of multiple myeloma—an incurable B-cell malignancy that originates from plasma cells (1)—prompted to test different molecules as therapeutic targets (2).

We described that protein kinase CK2 is crucial for multiple myeloma cell survival, positively regulates STAT3 and NF-κB signaling, and controls multiple myeloma cell sensitivity to melphalan (3). Indeed, CK2 critical role in maintaining the oncogenic phenotype suggests that it could be an optimal therapeutic target (4). Phase I clinical trials with the oral CK2 inhibitor CX-4945 (Cylene Pharmaceuticals; ref. 5) are ongoing in patients with multiple myeloma (trial number: NCT01199718).

The molecular chaperone HSP90 plays a pivotal role in protein folding, maturation, and cell survival (6). Multiple myeloma plasma cells are exquisitely sensitive to cytotoxicity of HSP90 inhibitors such as geldanamycin and its derivatives (7–11). Interestingly, CK2 regulates the activity of the chaperone complex formed by CDC37 and HSP90 by phosphorylating Ser13 on CDC37 (12). This phosphorylation promotes the association of HSP90 with client proteins, in particular protein kinases (13). HSP90 takes part in the endoplasmic reticulum (ER) stress–induced unfolded

Authors' Affiliations: [1]Department of Medicine, Clinical Immunology and Hematology Branches; [2]Venetian Institute of Molecular Medicine, Centro di Eccellenza per la Ricerca Biomedica; [3]Department of Biological Chemistry, University of Padova, Padova; and [4]Medical Oncology Unit, Magna Graecia University, Catanzaro, Italy

Note: Supplementary data for this article are available at Clinical Cancer Research Online (http://clincancerres.aacrjournals.org/).

Corresponding Authors: Francesco Piazza, Department of Medicine, University of Padova, Via Giustiniani 2, Padova 35128, Italy. Phone: 0039-049-821-2298; Fax: 0039-049-821-1970; E-mail: francesco.piazza@unipd.it; and Gianpietro Semenzato, E-mail: g.semenzato@unipd.it

doi: 10.1158/1078-0432.CCR-11-1789

Published OnlineFirst February 20, 2012; DOI:10.1158/1078-0432.CCR-11-1789

Translational Relevance

Together with aberrantly active signal transduction pathways, a central role in multiple myeloma pathogenesis is played by the chaperoning system of HSP and by the endoplasmic reticulum (ER) stress/unfolded protein response (UPR), which are able to render multiple myeloma cells resistant to proapoptotic stresses. Clinically, this could contribute to multiple myeloma cell resistance to conventional and novel agents, which is the main obstacle to the eradication of this disease. Clinical trials are investigating whether targeting HSP or UPR with novel compounds could increase the sensitivity of multiple myeloma cells to cytotoxic agents. Protein kinase CK2 supports multiple myeloma cell growth by upregulating several signaling pathways. This kinase might be important for HSP90 function, and oral inhibitors are under investigation in phase I clinical trials in multiple myeloma. Showing whether CK2 crosstalks with HSP90 and UPR in multiple myeloma will improve the knowledge on multiple myeloma biology and may pave the way to design novel and more effective therapies for this disease.

protein response (UPR) in multiple myeloma cells (14, 15). The UPR is mediated by conserved signaling pathways aimed at coping with unfolded protein load in the ER (16). The UPR can end up in a compensatory response; however, if ER stress is prolonged or too intense, apoptosis occurs (17). ER stress sensors initiating the UPR are the kinase/endoribonuclease IRE1α, the kinase PERK, and the transcription factor ATF6, which are kept inactivated by the ER chaperone BIP/GRP78. Unfolded proteins accumulating in the ER attract BIP/GRP78 and the sensors start their signaling cascades. IRE1α oligomerizes, autophosphorylates, and excises an intron from *XBP1* mRNA. Unspliced XBP1 (XBP1u) is converted to a larger spliced XBP1 (XBP1s) protein, a transcription factor–activating genes involved in UPR and ERAD (ER-assisted degradation), including *BIP/GRP78* itself. PERK is a Ser/Thr protein kinase, which phosphorylates the translation regulator EIF2α, resulting in a reduction of mRNA translation and protein load in the ER. ATF6 translocates to the Golgi apparatus and is cleaved by proteases in an active form, which upregulates, among others, *BIP/GRP78*, *PDI*, and *EDEM1* transcription, resulting in increased ER chaperone activity and degradation of misfolded proteins. The transcription factor CHOP is induced downstream all the 3 UPR sensors (18, 19). The critical importance of the UPR for normal and malignant plasma cells is highlighted by a number of studies (20, 21). Recently, CK2 has been shown to control the ER stress response in prostate cancer cells (22); however, whether the CK2/HSP90/CDC37 axis could take part in the UPR in plasma cells is presently unknown.

Here, we present data involving CK2 in UPR and suggesting that its inhibition could represent an effective therapeutic strategy to be exploited alone or in combination with ER stress/UPR pathways manipulation in multiple myeloma.

Materials and Methods

Patients and cell cultures

To obtain patient samples, informed consent was achieved according to the Declaration of Helsinki. The internal Institutional Board approved the use of human material. Normal peripheral blood mononuclear cells (PBMC); malignant $CD138^+$ plasma cells; multiple myeloma cell lines RPMI-8226, U-266, and H-929; and the human stromal cell line HS-5 were isolated and cultured as described previously (23). Primary mesenchymal bone marrow stromal cells from patients with multiple myeloma were obtained as described previously (24). The interleukin (IL)-6–dependent multiple myeloma cell line INA-6—cultured in RPMI-1640 supplemented with 10% FBS and IL-6 (5 ng/mL)—was a gift of Dr. M. Gramatzki, University of Kiel, Kiel, Germany. Cocultures of HS-5 and INA-6 were stabilized as previously described (25).

Cytokines and chemicals

IL-6, tunicamycin, and thapsigargin were purchased from Sigma-Aldrich. K27 (2-amino-4,5,6,7-tetrabromo-1*H*-benzimidazole; see ref. 3); geldanamycin from Calbiochem-MERCK; tTBB (4,5,6,7-tetrabromo-1*H*-benzimidazole) from TOCRIS; and 17-AAG (17-*N*-allylamino-17-demethoxygeldanamycin) from LC Laboratories.

Assessment of drug concentration effect and calculation of the combination index

See supplementary file.

CK2 activity in cell lysates

CK2 activity was measured on the $R_3AD_2SD_5$ peptide substrate as previously described (26).

mRNA silencing

RNA interference was conducted as previously described (23), with siGLO green scrambled siRNAs, CK2α targeting siRNAs (100 pmoles) or the combination of the 2 (Dharmacon). CK2α target sequence was GCAUUUAGGUGGAGACUUC; GGAAGUGUGUCUUAGUUAC; GCUGGUCGCUUACAUCACU; and AACAUUGUCUGUACAGGUU.

Quantitative and qualitative PCR

See supplementary file.

Evaluation of growth and apoptosis

Apoptosis was assessed by Annexin V/propidium iodide staining (BD Pharmingen). Cells were labeled with Cy5 or fluorescein isothiocyanate (FITC)-Annexin V (Becton-Dickinson), allophycocyanin (APC)-conjugated anti-CD45 or anti-CD19, and phycoerythrin (PE)-Cy5–conjugated anti-CD38 (Becton-Dickinson). Fluorescence-activated cell-sorting (FACS) analysis was conducted using a FACSCalibur Cell Cytometer and the CellQuest Software (Becton-Dickinson).

Published OnlineFirst February 20, 2012; DOI:10.1158/1078-0432.CCR-11-1789

Human multiple myeloma xenograft murine model

See supplementary file.

Western blotting and immunoprecipitation

Western blotting was conducted according to standard protocols. Antibodies used were CK2α (3); PARP, IRE1α, BIP/GRP78, phospho-Ser51 EIF2α, and total EIF2α (Cell Signaling Technology); PERK, CHOP/GADD153, phospho-Ser13 CDC37, and phospho-Ser727 IRE1α (Abcam); phospho-Thr981 PERK, CDC37, and RS6K (Santa-Cruz Biotechnology); GAPDH (Ambion); β-actin (Sigma-Aldrich); and HSP90 (Enzo Life Sciences). Densitometric assay was conducted using the Quantity One Software (BioRad). Immunoprecipitation was conducted according to standard protocols, with IRE1α antibody (5 μg) and True blot anti-rabbit IgG immunoprecipitation beads. The true blot system was used to reveal the Immunoprecipitation bands (eBioscience).

Microsomal fraction preparation

Microsomal cellular subfractions were obtained as described previously (27).

Immunofluorescence and confocal microscopy

Experiments were carried out as previously described (3, 23). Antibodies used were CK2α together with Alexa Fluor 568 goat anti-rabbit (Molecular Probes Europe), SERCA 2 (Affinity Bioreagents) together with Alexa Fluor 488 goat anti-mouse. DAPI (4′,6-diamidino-2-phenylindole) staining detected the cell nuclei.

Statistical analysis

Data obtained were evaluated for their statistical significance with the 2-tailed paired Student *t* test or ANOVA. Values were considered statistically significant at *P* values below 0.05.

Results

CK2 partly localizes to the ER and its kinase activity is increased in multiple myeloma cells upon ER stress

The ER stress/UPR is an essential determinant of normal and malignant plasma cell fate (21, 28). We asked whether CK2, as an essential molecule for multiple myeloma cell survival (3), could be involved in the ER stress/UPR in multiple myeloma cells.

First, we checked whether CK2α (the catalytic subunit of this protein kinase) could localize to the ER in U-266, INA-6 cells, and freshly isolated normal PBMCs by confocal immunofluorescence microscopy. The sarcoplasmic/ER Ca^{++}-ATPase (SERCA) protein was used as an ER-specific control. As shown in Fig. 1A, CK2α localized mainly in the cytoplasm, in both the multiple myeloma cell lines. SERCA staining was evident in discrete areas of the cell corresponding to the ER. A significant fraction of CK2α localized close to SERCA-rich areas (yellow fluorescence in the merge images) suggesting that a pool of this kinase lies in the ER. In normal PBMCs, we observed a similar pattern of CK2α staining and, even if at a lesser extent than in multiple myeloma cells, an evident CK2α-SERCA colocalization.

Next, we investigated whether CK2 activity could be influenced by ER stress. To this aim, we treated U-266 and H-929 multiple myeloma cells (not shown) with the ER stress inducer thapsigargin. As shown in Fig. 1B, thapsigargin caused an increase of CK2 kinase activity against a synthetic peptide (see Materials and Methods for details) in a time-dependent manner ($P = 0.014$ for the 6-hour and $P = 0.020$ for the 24-hour time point). Moreover (top right), thapsigargin caused increased Ser13 CDC37 phosphorylation, which is a well-known CK2 substrate (12). We also checked whether ER stress could change CK2 intracellular localization assuming that this kinase could concentrate in the ER. However, Western blot analysis of CK2α in the microsomal (marked by high rS6 kinase expression) and cytosolic [with high glyceraldehyde-3-phosphate dehydrogenase (GAPDH) levels] cellular subfractions did not show significant changes of CK2 distribution upon ER stress induction (Fig. 1B, bottom right). These observations indicate that ER stress induces CK2 activity without modifying its ER-specific localization.

CK2 inactivation in multiple myeloma cells affects the ER stress/UPR signaling cascades

We next investigated whether inhibition of CK2 activity could affect the main ER stress–induced UPR signaling cascades. To this aim, we treated U-266 multiple myeloma cells with the selective, ATP-competitive CK2 chemical inhibitor K27 for 18 hours. We used the inhibitor at different concentrations, according to our previously published dose–response tests (3). K27 is a TBB derivative (29) displaying a fairly good specificity for CK2 at the concentration used here. However, as shown in the work of Sarno and colleagues (29), at higher concentrations (10 μmol/L and higher), it is possible that K27 has off-target effects toward other kinases. Interestingly, Western blot analysis of control and K27-treated U-266 cells revealed significant modifications of the main UPR regulating signaling molecules upon K27: a strong reduction of IRE1α, a reduction of BIP/GRP78 and CHOP/GADD153 protein levels, and an increase of phospho-Ser51 EIF2α levels (Fig. 1C). To validate these findings, we carried out RNA interference experiments to down-regulate CK2α levels in U-266 cells. As shown in Fig. 1D, Western blot analysis confirmed that CK2α was efficiently knocked down upon nucleofection of U-266 cells with specific siRNAs [the densitometric analysis showed about a 50% protein level reduction (graph at the bottom); densitometry value $= 0.53 \pm 0.03$ (SEM) over the control, $P < 0.05$, $n = 12$]. CK2α knocked down multiple myeloma cells displayed alterations of the UPR-related proteins similar to those observed in the conditions of CK2 chemical inhibition. We therefore checked the EIF2α upstream kinase PERK, and, remarkably, we could detect that CK2α silencing caused increased phosphorylation of PERK at Thr981. However, in CK2α-silenced samples, we could not detect a significant reduction of

Published OnlineFirst February 20, 2012; DOI:10.1158/1078-0432.CCR-11-1789

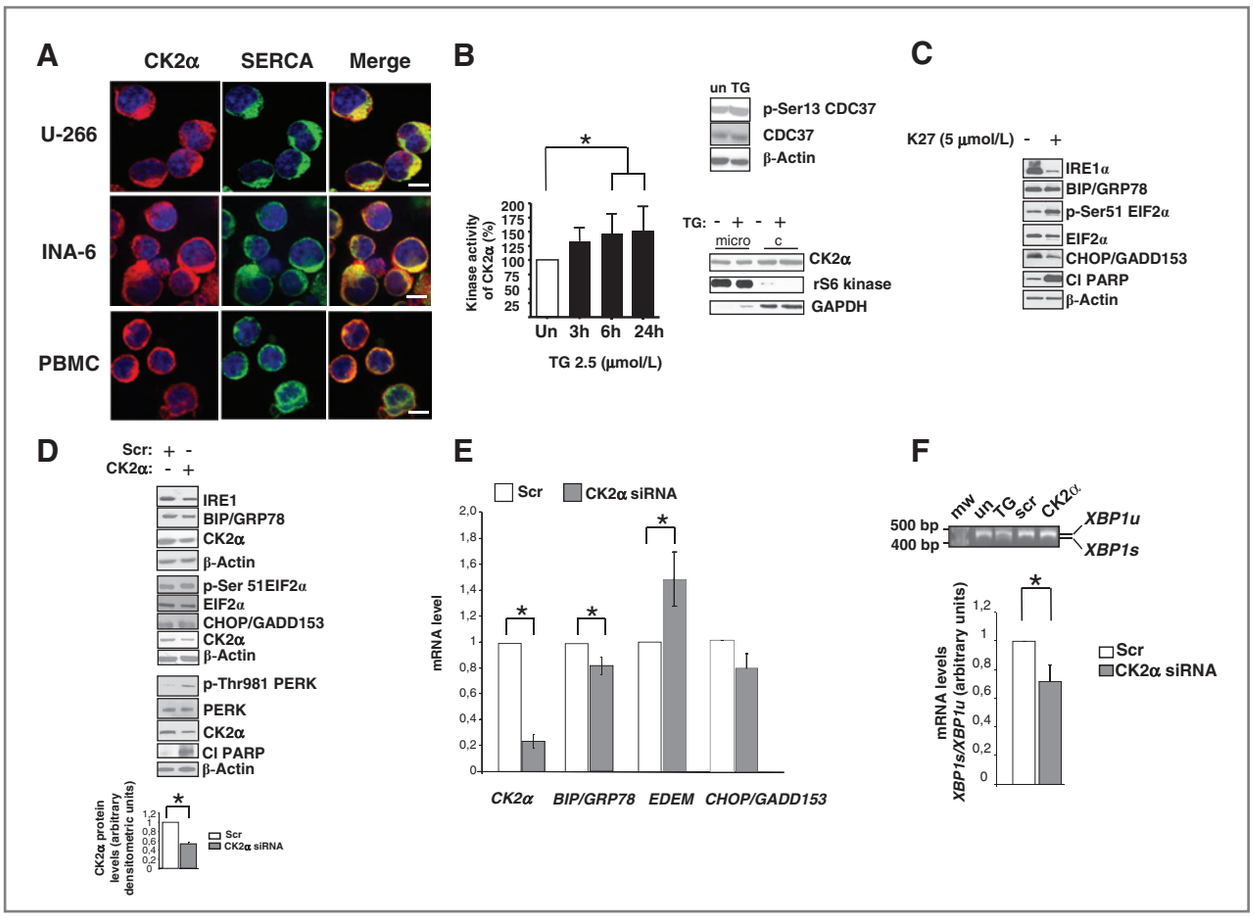

Figure 1. CK2α kinase activity is modified during ER stress and the main UPR signaling pathways are altered upon CK2α inactivation/downregulation in multiple myeloma cells. A, immunofluorescence analysis of CK2α cellular localization in multiple myeloma cells and normal PBMCs. U-266 (top), INA-6 (middle) cells, and PBMCs from healthy donors (bottom) were stained with antibodies recognizing CK2α (red) and SERCA 2b (green) and confocal microscopy was conducted. Nuclei are stained with DAPI (blue). For all the images: 600× magnification, oil objective, room temperature. Scale bar, 10 μm. B, total CK2α kinase activity was measured by *in vitro* kinase assay against a synthetic peptide (left graph) in U-266 cells, untreated (white bar, un), or upon incubation with thapsigargin (TG) at 2.5 μmol/L for 3, 6, and 24 hours (dark bars) and by Western blot analysis of phospho-Ser13 CDC37 (p-Ser13 CDC37, top right) upon thapsigargin treatment for 6 hours. Western blot analysis (bottom right) of CK2α, rS6 kinase, and GAPDH in the microsomal (micro) and cytosolic (c) fractions of control or thapsigargin-treated (2.5 μmol/L) U-266 cells for 6 hours. *, $P < 0.05$. C–E, expression of the main UPR signaling molecules and of cleaved (Cl.) PARP was measured by Western blotting (C and D) or quantitative RT-PCR (E) in U-266 cells treated with K27 (5 μmol/L) for 18 hours (C) or after CK2α knockdown through nucleofection of U-266 cells with CK2α-directed siRNA oligonucleotides for 72 hours (D and E). The molecules measured are listed in the figure (p-Ser51 EIF2α, phosphorylated Ser51 EIF2α; p-Thr981 PERK, phosphorylated Thr981 PERK). Downregulation of CK2α protein levels was measured by Western blotting followed by densitometric analysis (D) or quantitative real-time PCR (E). β-Actin was used as a loading control. The relative amounts of mRNA were determined by normalization for β-actin expression. *, $P < 0.05$. F, mRNA expression of *XBP1s/XBP1u* in U-266 cells treated with CK2α-directed siRNA oligonucleotides. The relative amount of *XBP1s/XBP1u* was determined by PCR. Top, agarose gel of the *XBP1s/XBP1u* PCR products of U-266 cells nucleofected with scramble and CK2α-directed siRNA oligonucleotides for 72 hours. U-266 cells treated with thapsigargin (2.5 μmol/L) for 6 hours were used as ER stress control. Quantification of the bands was conducted using the gene scan fragment length analysis (bottom). *, $P < 0.05$. mw, molecular weight; Scr, scrambled.

CHOP/GADD153 protein levels. Finally, the levels of IRE1α phosphorylated on Ser724, which are dependent on IRE1α kinase activity itself, did not change upon CK2 inhibition either with K27 or RNA interference and were barely detectable under these conditions (Supplementary Fig. S1A and S1B). Of note, both K27 and CK2α knockdown with siRNAs were accompanied by PARP cleavage, confirming the essential role of CK2 for multiple myeloma cell survival.

Next, we checked the transcriptional program set up by the ER stress/UPR pathways upon CK2α silencing. To this aim, we conducted quantitative PCR analysis of mRNA expression of direct UPR target genes, namely, *BIP/GRP78*, *EDEM*, and *CHOP/GADD153*, on cDNA extracted from U-266 cells nucleofected with control or CK2α-directed siRNA oligonucleotides. As shown in Fig. 1E, *CK2α* mRNA levels were significantly reduced in these experiments. We observed a significant reduction of expression for *BIP/GRP78* and an increase for *EDEM* in the CK2α-silenced samples ($P < 0.05$, $n = 4$), whereas there was no statistically sizeable difference for *CHOP/GADD153* (although a trend toward reduced levels could be appreciated). We

Published OnlineFirst February 20, 2012; DOI:10.1158/1078-0432.CCR-11-1789

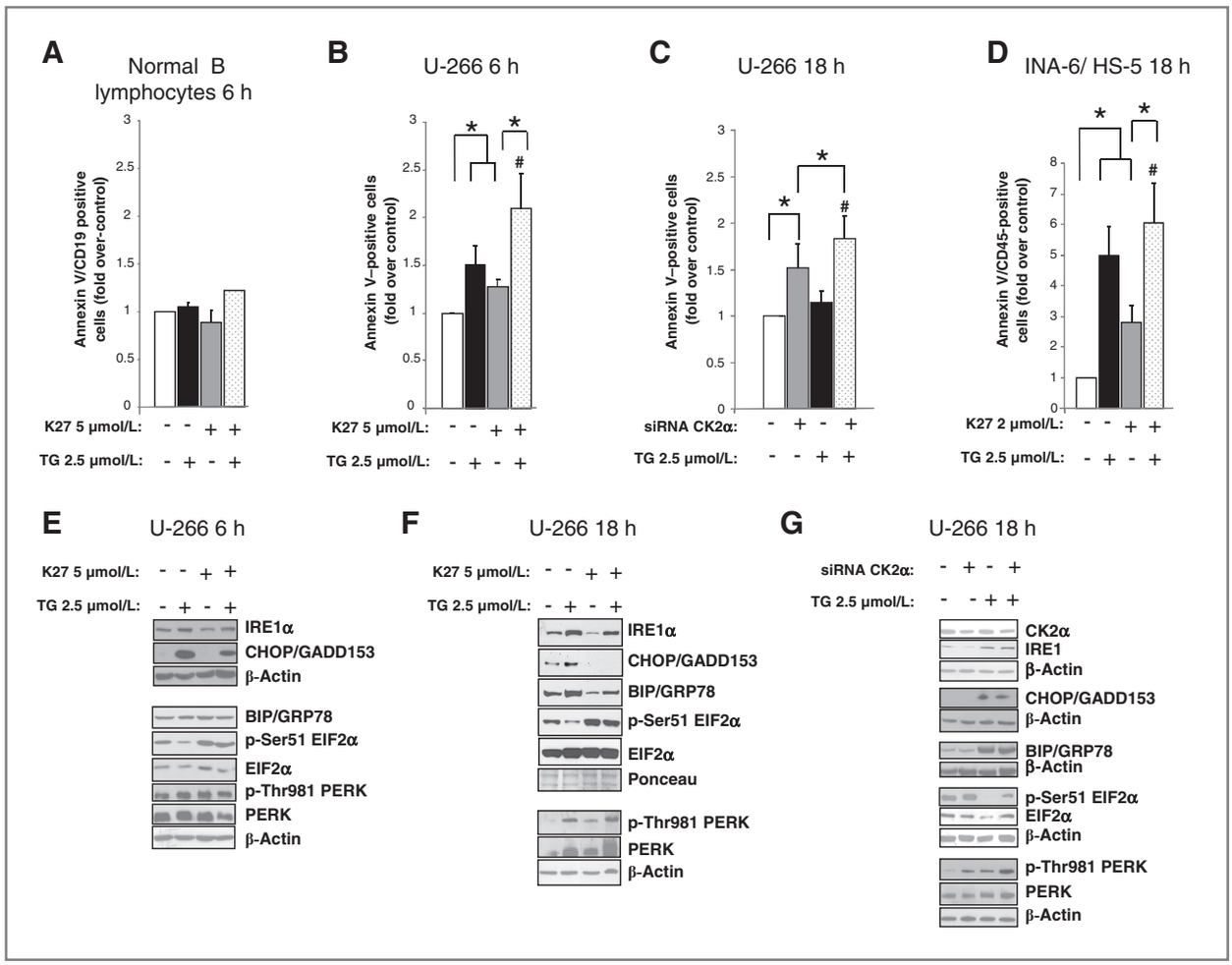

Figure 2. Induction of ER stress and inactivation/downregulation of CK2α synergizes in inducing apoptosis and affect expression of the main UPR branches. A–D, apoptosis was assessed with Annexin V staining and FACS analysis in normal $CD19^+$ B lymphocytes (A) or U-266 cells (B) untreated (white bars) or treated with 2.5 μmol/L thapsigargin (TG; dark bars), K27 (5 μmol/L; gray bars), or the combination of the 2 molecules (gray dotted bars) for 6 hours, in U-266 cells nucleofected with CK2α-directed siRNA oligonucleotides for 72 hours and subsequently treated with 2.5 μmol/L thapsigargin for 18 hours (C) or in cocultures of INA-6/HS-5 cell lines treated with 2 μmol/L K27, 2.5 μmol/L thapsigargin, or the combination of the 2 compounds for 18 hours (D). Data represent mean ± SEM of at least $n = 3$ experiments. *, $P < 0.05$; #, $P < 0.05$ between samples treated with 2.5 μmol/L thapsigargin alone and thapsigargin (2.5 μmol/L) together with K27 (5 μmol/L; A, B, D) or siRNA for CK2α (C). E–G, expression of the main UPR signaling molecules are evaluated through Western blot analysis in U-266 cells treated with K27 (5 μmol/L), thapsigargin (2.5 μmol/L) or the combination of the 2 compounds for 6 hours (E) or 18 hours (F) or, in separate experiments, in U-266 cells nucleofected with CK2α-directed siRNAs for 72 hours and subsequently treated with thapsigargin (2.5 μmol/L) for 18 hours (G). Antibodies used are listed in the figure.

also determined the amount of *XBP1s* (spliced) over *XBP1u* (unspliced), which measures IRE1α-dependent endoribonuclease activity under ER stress conditions. XBP1 is a transcription factor essential for plasma cell development (28) and whose overexpression is associated with myelomagenesis (21). In agarose gel, the *XPB1s* band was appreciated upon thapsigargin stimulation; however, it was undetectable under CK2α RNA interference (Fig. 1F, top); nonetheless, a more sensitive quantification of the relative amounts of *XBP1s*/*XBP1u*—through the gene scan fragment length analysis technique—showed that *XBP1s* over *XBP1u* is significantly reduced under inhibition of CK2α by RNA interference, as compared with scrambled nucleofected controls (Fig. 1F, bottom; $P < 0.05$, $n = 6$).

CK2 protects from thapsigargin-induced multiple myeloma cell apoptosis and mediates the activation of UPR pathways

We next asked whether ER stress–induced multiple myeloma cell apoptosis could be influenced by CK2 inactivation. First, we looked at survival of normal B lymphocytes and multiple myeloma cells by Annexin V staining upon thapsigargin, K27, or thapsigargin plus K27 treatment for 6 and 18 hours. As shown in Fig. 2A, normal B lymphocytes were unaffected by the treatment with thapsigargin and K27 for 6 hours. On the contrary, both thapsigargin and K27 were able to induce a significant amount of apoptosis of U-266 cells after 6 hours. Thapsigargin-induced apoptosis was stronger at 18 hours (data not shown). Remarkably, the

Published OnlineFirst February 20, 2012; DOI:10.1158/1078-0432.CCR-11-1789

treatment with the 2 molecules in combination caused a statistically significant higher level of apoptosis, as compared with the single treatments ($P < 0.05$, $n = 4$), only in malignant plasma cells (Fig. 2B). This effect lasted up to 18 hours (data not shown). Furthermore, RNA interference experiments confirmed that also CK2α silencing, coupled with thapsigargin treatment, led to a significantly higher rate of cell death than the single conditions (Fig. 2C; $P < 0.05$, $n = 4$). Finally, the cooperation between CK2 inhibition and thapsigargin treatment was evident even on INA-6 multiple myeloma cells ($CD45^+$) grown in the protective presence of HS-5 bone marrow stromal cells ($CD45^-$), a model, which reproduces some features of the multiple myeloma *milieu* (see Materials and Methods; Fig. 2D; $P < 0.05$, $n = 4$). Here, K27 was used at a lower concentration (2 μmol/L), due to the higher sensitivity of INA-6 cells to CK2 inhibitors that we observed in dose–response assays (not shown). Western blot analysis on U-266 multiple myeloma cells treated with thapsigargin and K27 for 6 and 18 hours (Fig. 2E and F) showed that thapsigargin induced an increase of IRE1α, CHOP/GADD153, and BIP/GRP78 levels oppositely than CK2 inhibition with K27, which led to a reduction of the 3 proteins (more evident at 18 hours). Thapsigargin and K27 caused an increase of phospho-Thr981 PERK. Remarkably, in the combined treatment with thapsigargin plus K27, thapsigargin-induced increase of IRE1α, BIP/GRP78, and CHOP/GADD153 was attenuated or even abolished by K27, whereas the elevation of phospho-Thr981 PERK remained unaffected. We also carried out RNA interference experiments and thapsigargin treatment. CK2α silencing alone showed similar changes to those observed with K27. In the combined treatment, we observed an analogous pattern of changes, even though to a lesser extent as than K27 (Fig. 2G). Altogether, these data suggest that CK2 protects from ER stress–induced apoptosis and sustains a specific UPR by upregulating IRE1α level and downregulating PERK activity in multiple myeloma cells.

HSP90 inhibition and CK2 inactivation have a synergic cytotoxic effect on multiple myeloma cells

CK2 regulates the HSP90-CDC37 molecular chaperone by phosphorylating CDC37 on Ser13 (12, 13). HSP90 regulates the ER stress/UPR pathways in multiple myeloma cells (14, 15). Because we observed that CK2 is involved in the ER stress–induced apoptosis in multiple myeloma cells, we next investigated whether CK2 and HSP90 could cross-talk in sustaining multiple myeloma cell growth.

First, we hypothesized that the simultaneous inhibition of CK2 and HSP90 could cause either an additive or a synergic effect in terms of multiple myeloma cell apoptosis. To test this idea, we treated U-266 multiple myeloma cells with increasing doses of K27 (range, 1–15 μmol/L) or of HSP90 inhibitor geldanamycin (range, 0.05–5 μmol/L), evaluated the rate of inhibition of cell proliferation by ^{3}H-thymdine incorporation assay, and calculated the IC_{50} for the 2 agents (geldanamycin, 0.19 μmol/L; K27, 6.98 μmol/L). Then, we conducted the constant ratio drug combination assay (see details in Supplementary Materials and Methods) and found that the combination index was 0.291, indicating a strong synergism between K27 and GA (Fig. 3A). Next, we tested whether apoptosis could be involved in this synergy. Normal B lymphocytes or U-266 and RPMI-8226 cells were treated with 2 increasing doses of geldanamycin (0.15 and 0.5 μmol/L), K27 (5 μmol/L), or the combination of the two for 3 and 6 hours and the rate of apoptosis was evaluated. The percentage of Annexin V–positive cells after 3 hours did not change significantly upon the different treatments in normal cells as well as both the multiple myeloma cell lines (not shown). At later time points (6 hours), while geldanamycin and K27 single treatments did not affect normal lymphocyte viability (Fig. 3B), they clearly caused apoptosis of malignant plasma cells (Fig. 3C and D); remarkably, the combined treatment with the 2 drugs still did not affect normal B-cell survival ($P > 0.05$, $n = 3$), whereas it triggered a higher rate of multiple myeloma cell apoptosis than the single treatments ($P < 0.05$, $n = 3–5$). Next, we assessed the anti-myeloma effect of HSP90 and CK2 inhibition in the presence of bone marrow stromal cells. INA-6 cells were cultured with HS-5 cells in the presence of geldanamycin (0.15 μmol/L), K27 (2 μmol/L), and with the combination of both compounds. As shown in Fig. 3E, the addition of geldanamycin and K27 as single agents to INA-6 cells grown alone resulted in a statistically significant increase of the rate of apoptosis compared with untreated samples. Remarkably, the same or even more pronounced effect was seen in coculture experiments of INA-6 cells ($CD45^+$) grown with HS-5 stromal cells ($CD45^-$; Fig. 3F) or with patients with multiple myeloma–derived mesenchymal stromal cells (Fig. 3G), as judged by the higher percentage of $CD45^+$/Annexin V–positive cells than in untreated samples. Strikingly, the combination of CK2 and HSP90 inhibitors caused a much higher rate of apoptosis than the single inhibition of the 2 molecules ($P < 0.05$, $n = 4$), in all the conditions. Western blot analysis of cleaved PARP protein levels validated all these results (Supplementary Fig. S2A). Finally, we assayed whether the synergy of CK2/HSP90 inhibitors was present also on primary malignant plasma cells from patients. To this aim, $CD138^+$ plasma cells from 8 patients with multiple myeloma (see Table 1 for clinical details) were treated with geldanamycin (0.15 μmol/L), K27 (2 μmol/L), or the combination of the 2 for 18 hours. Figure 3H summarizes the data obtained. Each compound determined apoptosis, which was significantly greater upon combination of both drugs ($P < 0.05$, $n = 8$). We also carried out RNA interference experiments. Control or CK2α-silenced U-266 cells were exposed to HSP90 inhibition with geldanamycin (0.15 or 0.5 μmol/L) for 6 hours. Exposure to geldanamycin of CK2α-silenced multiple myeloma cells led to higher cytotoxicity than the single HSP90 inhibition or CK2α silencing (Fig. 3I; $P < 0.05$, $n = 5$). CK2α silencing was confirmed by quantitative reverse transcriptase RT-PCR analysis of mRNA expression (not shown) as well as PARP cleavage and reduction of CK2α protein levels by Western blot analysis (Supplementary Fig. S2B).

Published OnlineFirst February 20, 2012; DOI:10.1158/1078-0432.CCR-11-1789

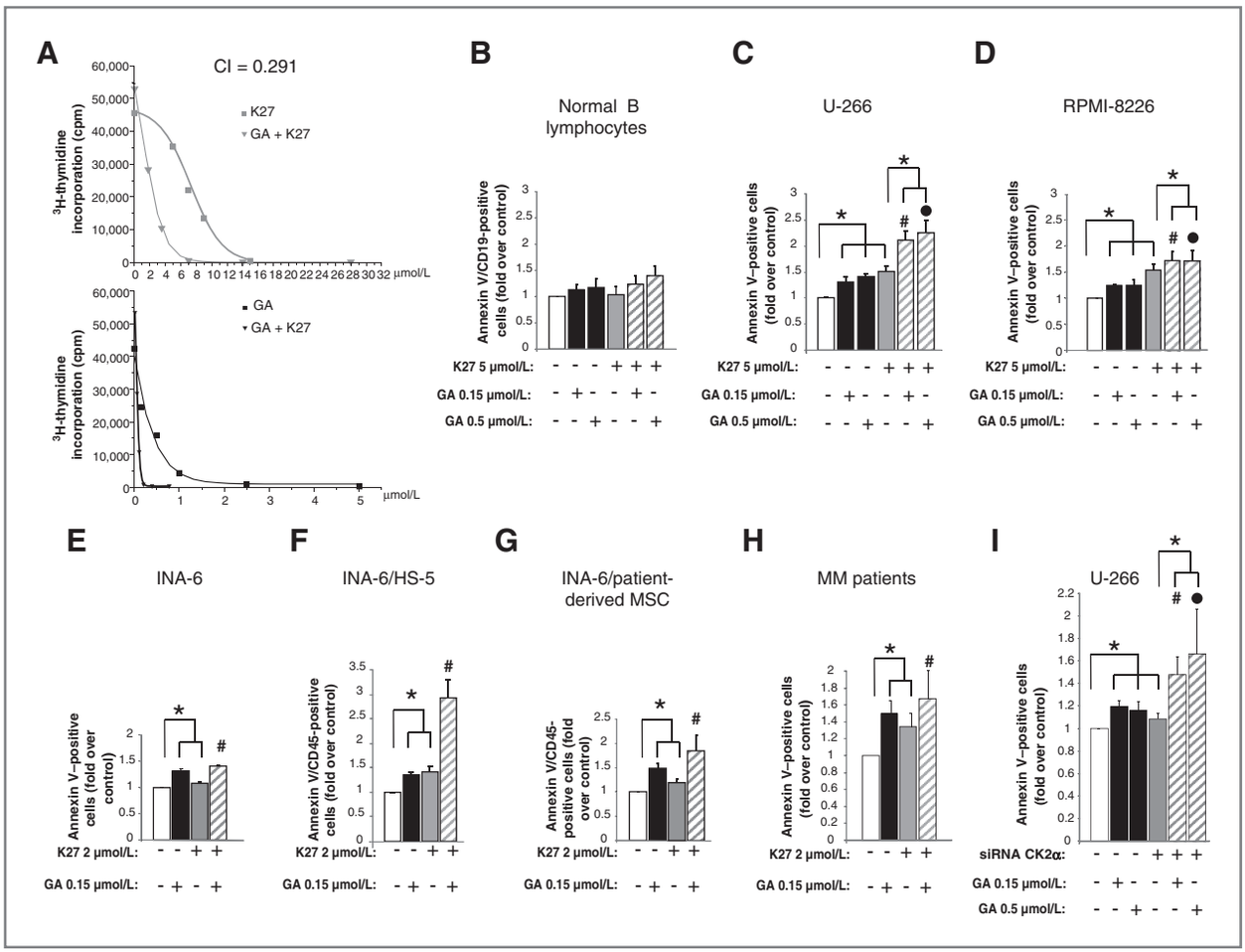

Figure 3. Effects of CK2α inactivation and HSP90 inhibition on multiple myeloma cell survival. A, synergistic effect of K27 and geldanamycin (GA) on U-266 cell proliferation. Top graph, dose–response of U-266 incubated for 48 hours with increasing concentrations of K27 alone (gray squared curve) or K27 plus GA (gray triangle curve); bottom graph, dose–response of U-266 incubated for 48 hours with increasing concentrations of GA alone (black squared curve) or K27 plus GA (black triangle curve). Cell proliferation was assessed by ^{3}H-thymidine incorporation assay. IC_{50} for K27 was calculated as 6.98 μmol/L and for GA as 0.19 μmol/L. The combination index (CI), obtained according to the formula described in the Materials and Methods section, was calculated as to be 0.291, indicating a synergic effect of K27 with GA. B–D, quantification of apoptosis through Annexin V staining and FACS analysis in normal CD19$^+$ B lymphocytes (B), U-266 (C), and RPMI-8226 (D) multiple myeloma cell lines exposed to different concentrations of the HSP90 inhibitor GA (0.15 or 0.5 μmol/L, dark bars), the CK2 inhibitor K27 (5 μmol/L), or the combination of both (gray striped bars) for 6 hours. E–G, histogram plots summarizing Annexin V staining and FACS analysis of INA-6 multiple myeloma cells cultured alone (plus IL-6, 5 ng/mL; E) or in co-cultures with the human bone marrow stroma cell line HS-5 (F) or patients with multiple myeloma–derived mesenchymal stromal cells (MSC; G) and treated with K27 (2 μmol/L), GA (0.15 μmol/L), or the combination of the 2 compounds for 18 hours. Experiments were carried out by staining with APC-conjugated anti-CD45 antibody, which is expressed by INA-6 cells but not by stromal cells and with FITC-conjugated Annexin V. H, representative histogram summarizing FACS analysis of CD38-positive plasma cells derived from patients with multiple myeloma (MM) treated with GA (0.15 μmol/L), K27 (2 μmol/L), or the combination of the 2 compounds for 18 hours. Experiments were carried out by staining with PE-Cy5–conjugated anti-CD38 antibody, which is expressed by multiple myeloma plasma cells and FITC-conjugated Annexin V. B–H, data represent mean ± SEM. *, $P < 0.05$; #, $P < 0.05$ between samples treated with GA (0.15 μmol/L) alone and GA (0.15 μmol/L) together with K27 at the concentration indicated in the figure; •, $P < 0.05$ between samples treated with GA (0.5 μmol/L) alone and GA (0.5 μmol/L) together with K27. I, apoptosis measured with Annexin V staining analysis in U-266 cells nucleofected with scramble siRNA oligonucleotides (white and dark bar) or CK2α-directed siRNA oligonucleotides and treated with GA (0.15 μmol/L) or GA (0.5 μmol/L; gray striped bars) for 6 hours. Data represent mean ± SEM. *, $P < 0.05$; #, $P < 0.05$ between scramble oligonucleotide nucleofected cells treated with GA (0.15 μmol/L) and cells nucleofected with CK2α-directed siRNA oligonucleotides treated with GA (0.15 μmol/L). •, $P < 0.05$ between scramble oligonucleotide nucleofected cells treated with GA (0.5 μmol/L) and cells nucleofected with CK2α-directed siRNA oligonucleotides treated with GA (0.5 μmol/L).

In vivo anti-myeloma effects of CK2 inhibition

To solidify our results obtained with multiple myeloma cells lines and cells from patients with multiple myeloma, we set up an *in vivo* mouse xenograft multiple myeloma model by subcutaneous injection of U-266 cells in CB17-SCID mice. Mice were randomized to receive the vehicle, the CK2 inhibitor tTBB (which is structurally closely related to K27 of which it is the precursor; ref. 26), and tTBB plus the HSP90 inhibitor 17-AAG. Tumor volume was measured every day up to 32 days. As shown in Supplementary Fig. S3, tTBB caused a marked reduction of tumor growth as compared with the vehicle-receiving control group ($P < 0.05$ at

Published OnlineFirst February 20, 2012; DOI:10.1158/1078-0432.CCR-11-1789

Table 1. Disease features of patients from whom malignant plasma cells were obtained

Sample	Paraprotein type	First-line therapy	Response	Second-line therapy	Response	BZ resistance	Notes
MM1	IgGL	V-MP × 8	PRO	REV-DEX × 8	Therapy ongoing	Yes	
MM2	IgAK	V-MP × 9	PRO	REV-DEX × 1, Cyclo, CRD × 4	PRO	Yes	
MM3	MM micromolecular light chain L	VEL-DEX × 1	toxic death			NA	
MM4	MM micromolecular light chain L	V-MP × 6	VGPR			No	
MM5	IgDL (PCL)	VEL-DEX × 1	PRO	PAD	PRO	Yes	Transformation in plasmoblastic lymphoma
MM6	IgGK	MP × 7	PR			NA	Progression
MM7	MM micromolecular light chain K	High-dose DEX	PRO	VEL-DEX × 1, THAL-DEX, MEL-DEX	PRO	NA	BZ only one cycle withdrawn due to skin toxicity
MM8	IgGK	VEL-DEX × 3, Cyclo, ASCT	PR	PAD, DCEP	VGPR	No	

Abbreviations: ASCT, autologous stem cell transplantation; CRD, cyclophosphamide, lenalidomide, dexamethasone; Cyclo, cyclophosphamide; DCEP, dexamethasone, cyclophosphamide, etoposide, cisplatin; MEL-DEX, melphalan, dexamethasone; MM, multiple myeloma; MP, melphalan, prednisone; PAD, bortezomib, liposomal doxorubicin, dexamethasone; PCL, plasma cell leukemia; PR, partial remission; PRO, progression; REV-DEX, lenalidomide, dexamethasone; THAL-DEX, thalidomide, dexamethasone; V-MP, bortezomib, melphalan, prednisone; VEL-DEX, bortezomib, dexamethasone; VGPR, very good partial remission.

day 32). Remarkably, the combined treatment with tTBB and 17-AAG appeared to provide higher antigrowth efficacy than tTBB alone ($P < 0.05$ at day 32). Overall, these data suggest that *in vivo* CK2 inhibition is able to cause a strong multiple myeloma cell growth arrest, which is potentiated by the simultaneous inhibition of HSP90.

CK2 regulates the HSP90-dependent UPR in multiple myeloma cells

Our data suggest that CK2 could regulate the UPR pathways through, at least, 2 means, that is, stabilization of IRE1α protein and inhibition of PERK. As these are 2 HSP90-modulated processes (30), we checked the effects of CK2 and HSP90 inhibition on the ER stress/UPR cascades in multiple myeloma cells.

To this aim, we looked at the expression of UPR proteins by Western blot analysis at different time lapses (3 and 6 hours) upon CK2, HSP90, or both protein inhibition. Treatment of U-266 and RPMI-8226 cells with geldanamycin caused a reduction of IRE1α protein levels, which began as early as after 3 hours (Supplementary Fig. S4A and S4B) and was more evident after 6 hours (Fig. 4A and B). Only in RPMI-8226, geldanamycin (0.5 μmol/L) caused an increase of BIP/GRP78 levels after 6 hours. In both cell lines geldanamycin caused a reduction of phospho-Ser51 EIF2α and, in U-266 cells, also of total and phospho-Thr981 PERK levels. These data are in line with previously published work (15). Remarkably, K27 markedly enhanced the geldanamycin-dependent reduction of IRE1α and caused a decrease of BIP/GRP78 at 6 hours, which was clear especially in RPMI-8226 cells and in U-266 cells at later time points (Fig. 1C, 18 hours). K27 to some extent opposed the geldanamycin-driven BIP/GRP78 increase (more evident at the mRNA level, as shown below). Moreover, in cells treated with the combination of the 2 agents, the K27-dependent increase of phospho-Ser51 EIF2α was minimally affected by the addition of geldanamycin, as was the increase of phospho-Thr981 PERK. Importantly, these changes of BIP/GRP78 and phospho-Ser51 EIF2α were also clearly seen in freshly isolated plasma cells from patients with multiple myeloma treated with geldanamycin, K27, or both agents (Fig. 4C). Experiments of RNA interference downregulating CK2α and treatment with geldanamycin for 3 (Supplementary Fig. S4C) and 6 hours (Fig. 4D), in part, reproduced the effects obtained with K27 on IRE1α and BIP/GRP78. Similarly, CK2α silencing slightly antagonized geldanamycin-induced reduction of phospho-Ser51 EIF2α, total and phospho-Thr981 PERK. Finally, we analyzed the IRE1α-triggered *XBP1s* mRNA formation upon treatment of multiple myeloma cells with geldanamycin, K27, or both. As shown in Fig. 4E, geldanamycin treatment led to *XBP1s* production only at very early time points (1 hour). At later time points (3 and 6 hours), in geldanamycin-treated samples, *XBP1s* disappeared, possibly due to IRE1α degradation and inactivation. CK2 inhibition with K27 seemed not to affect *XBP1* splicing at any time point and, when used with

Published OnlineFirst February 20, 2012; DOI:10.1158/1078-0432.CCR-11-1789

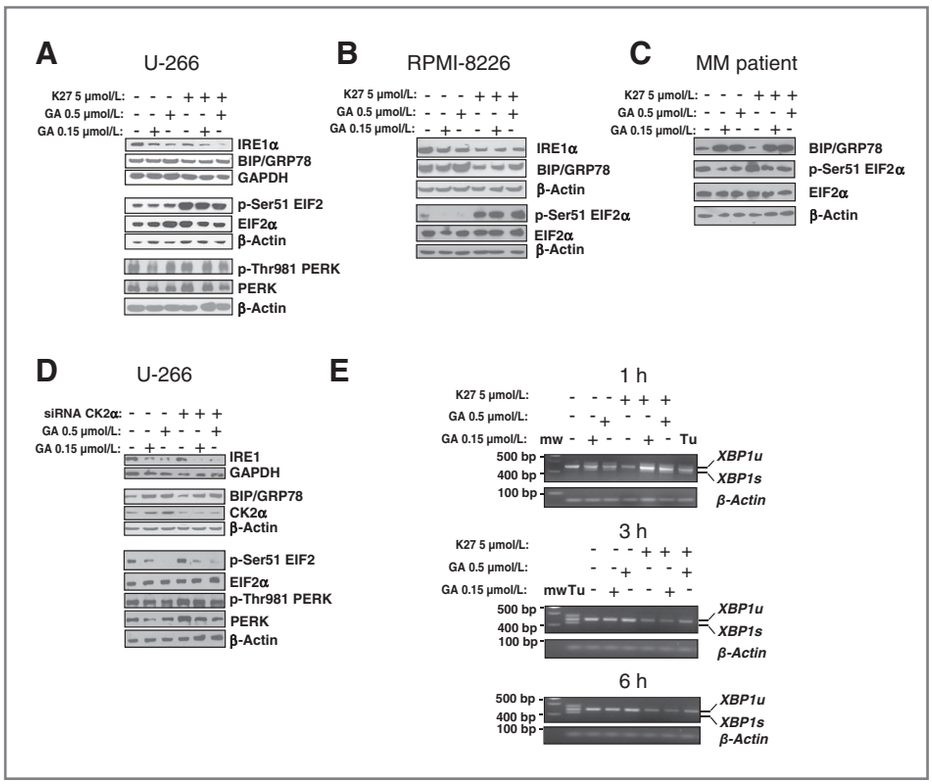

Figure 4. Effects of CK2α and HSP90 inhibition on the expression level of the main UPR-related proteins. U-266 (A) and RPMI-8226 cells (B) were treated with K27 (5 μmol/L) and geldanamycin (GA; 0.15 and 0.5 μmol/L) for 6 hours; patients with multiple myeloma (MM)-derived plasma cells (C) were treated with K27 (2 μmol/L) and GA (0.15 and 0.5 μmol/L) for 18 hours; U-266 cells were nucleofected with CK2α-directed siRNAs for 72 hours and subsequently treated with GA (0.15 and 0.5 μmol/L) for 6 hours (D). Expression levels of the main UPR signaling molecules were determined through Western blot analysis. Antibodies used are listed in the figure. E, U-266 cells were treated with K27 (5 μmol/L) and GA (0.15–0.5 μmol/L) for 1 hour (top), 3 hours (middle), or 6 hours (bottom) and *XBP1* splicing was determined by PCR. Cells treated with tunicamycin (Tu) for 6 hours were used as positive control for *XBP1s* formation. mw, molecular weight.

geldanamycin, did not result in changes of the geldanamycin-induced effects at 1 hour in agarose gel. However, similarly as for the data shown in Fig. 1F, assessment of *XBP1s* levels with the gene scan fragment length analysis revealed that K27 indeed caused a reduction of *XBP1s* (data not shown).

Transcription of UPR genes upon HSP90 inhibition is regulated by CK2

Next, we examined the consequences of CK2 inactivation on the geldanamycin-induced transcription of UPR-dependent genes, namely, *BIP/GRP78*, *EDEM*, and *CHOP/GADD153*, by quantitative real-time PCR. In a set of experiments, we treated U-266 cells with geldanamycin at increasing concentrations (0.15 and 0.5 μmol/L), K27 (5 μmol/L), or both. As shown in Fig. 5A, geldanamycin caused a dose-dependent increase of all the 3 target genes examined at 3 and 6 hours. K27 did not affect *BIP/GRP78* mRNA levels at these early time points (but it did reduce the protein at later time points; Fig. 1C), however, it triggered *EDEM* and, most noticeably, inhibited *CHOP/GADD153* transcription ($P < 0.05$, $n = 3$). Noteworthy, in the combination experiments, K27 strongly hampered the geldanamycin-induced increase of the target genes ($P < 0.05$, $n = 3$). In another set of experiments, CK2α was targeted by RNA interference and U-266 cells were exposed to geldanamycin for 3 and 6 hours (Fig. 5B). *CK2α* mRNA levels were reduced by 70% to 80% (data not shown). CK2α silencing led to a slight but significant reduction of *BIP/GRP78* and a more significant increase of *EDEM* mRNA. Remarkably, the geldanamycin-induced upregulation of *BIP/GRP78* mRNA expression was inhibited by CK2α knockdown. *CHOP/GADD153* mRNA was unaffected by CK2α knockdown; however, CK2α silencing effectively opposed its increase triggered by geldanamycin at 3 hours ($P < 0.05$).

Altogether, these data show that CK2α is needed for the HSP90-dependent IRE1α-mediated UPR in multiple myeloma cells.

CK2 inhibition causes a reduction of HSP90/CDC37/IRE1α complexes in multiple myeloma cells

CK2 controls the HSP90-dependent folding of client protein kinases through phosphorylation of Ser13 on its co-chaperone CDC37 and affects the formation of the macromolecular complex formed by CDC37, HSP90, and the client protein. We therefore tested whether the observed IRE1α reduction upon CK2 inhibition could be associated to decreased levels of HSP90/CDC37/IRE1α complexes. To this aim, we immunoprecipitated IRE1α from protein lysates of U-266 cells untreated or treated with K27 and analyzed the presence of HSP90, CDC37, and CK2 in the pulled-down complex by Western blot analysis. As shown in Fig. 6A, treatment with K27 caused a reduction of IRE1α, which was less abundant in the immunoprecipitate. Strikingly, while the amount of HSP90 and CDC37 co-immunoprecipitated with IRE1α was plentiful in the control samples, it was markedly reduced in the condition of CK2 blockade. Interestingly, CK2 was not found to co-immunoprecipitate with IRE1α, suggesting that the stability

Published OnlineFirst February 20, 2012; DOI:10.1158/1078-0432.CCR-11-1789

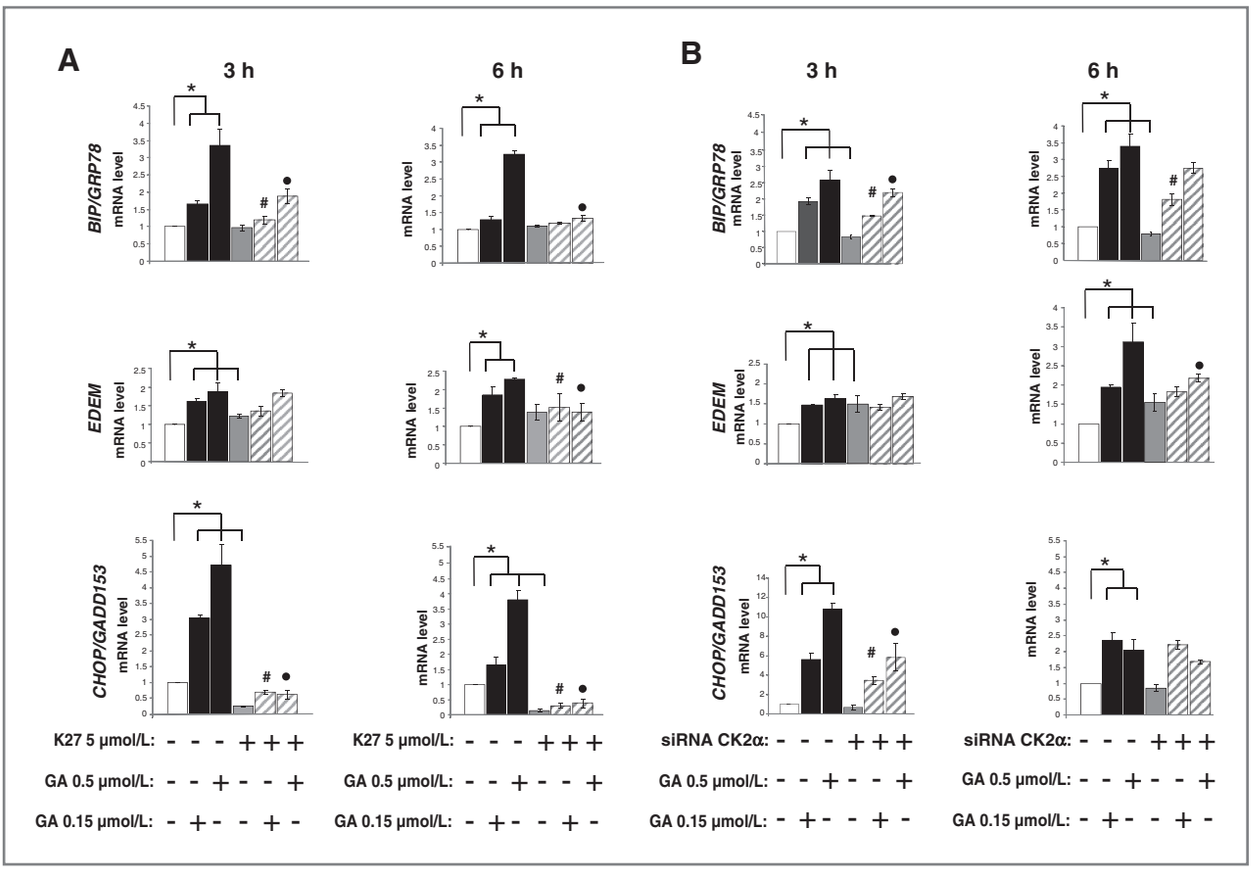

Figure 5. Effects of CK2α and HSP90 inhibition on *BIP/GRP78*, *EDEM*, and *CHOP* mRNA expression levels in U-266 cell. A, histograms showing *BIP/GRP78* (top), *EDEM* (middle), or *CHOP/GADD153* (bottom) mRNA levels assessed by quantitative RT-PCR as follows: U-266 cells grown in the absence (white bars) or presence of geldanamycin (GA; 0.15 μmol/L) or GA (0.5 μmol/L; black bars), of K27 5 μmol/L (gray bars), or the combination of the 2 molecules (gray striped bar), for 3 hours (left graphs) or 6 hours right graphs). B, same as in (A) with CK2α-directed siRNA to inactivate CK2 instead of K27. Data represent mean ± SEM of at least 3 independent experiments. *, $P < 0.05$; #, $P < 0.05$ between samples treated with GA (0.15 μmol/L) alone and GA (0.15 μmol/L) together with K27 (5 μ μmol/L; or siRNA for CK2α). ·, $P < 0.05$ between samples treated with GA (0.5 μmol/L) alone and GA (0.5 μmol/L) together with K27 (5 μmol/L; or siRNA for CK2α).

of HSP90–IRE1α interaction does not require a direct association of CK2 in the complex.

Discussion

We show here that protein kinase CK2 is activated by ER stress, lies upstream from IRE1α and PERK signaling branches, protects from ER stress–triggered apoptosis, and synergizes with HSP90 inhibition in inducing multiple myeloma cell growth arrest. Mechanistically, CK2 might control HSP90-dependent IRE1α protein stability and the extent of EIF2α phosphorylation.

CK2α localizes close to the ER (Fig. 1A). This finding in multiple myeloma cells extended previous reports in other cell types showing that CK2 localizes to the ER and phosphorylates ER-resident proteins (31–33). ER stress with thapsigargin increased CK2-specific activity (Fig. 1B). This observation is, to our knowledge, the first ever reported. Ablation of CK2 function resulted in a decrease of IRE1α and of BIP/GRP78 and in an increase of phospho-Thr981 PERK and phopsho-Ser51 EIF2α protein levels (Fig. 1C and D). This suggests that CK2 might inhibit PERK-mediated EIF2α phosphorylation at basal conditions. CK2 silencing led to a repression of *BIP/GRP78* and a stimulation of *EDEM* mRNA expression (Fig. 1E). *BIP/GRP78* and *EDEM* mRNA are upregulated following ER stress by the action of the IRE1α and ATF6 branches of the UPR, respectively (reviewed in ref. 34). Therefore, the reduction of IRE1α levels and of *XBP1s* upon CK2 inhibition could justify the decrease of the XBP1 target *BIP/GRP78*; on the other hand, the observed increase of the ATF6 target gene *EDEM* upon CK2 inhibition suggests that CK2 could restrain the ATF6-dependent signaling. Therefore, CK2 might regulate the UPR by maintaining IRE1α levels and buffering down PERK and ATF6 activity in multiple myeloma cells. Importantly, this type of homeostatic UPR has been associated with a compensatory, protective mechanism peculiar of plasma cells, in which by keeping the PERK-mediated axis buffered down and the IRE1α/XBP1-dependent defensive

Published OnlineFirst February 20, 2012; DOI:10.1158/1078-0432.CCR-11-1789

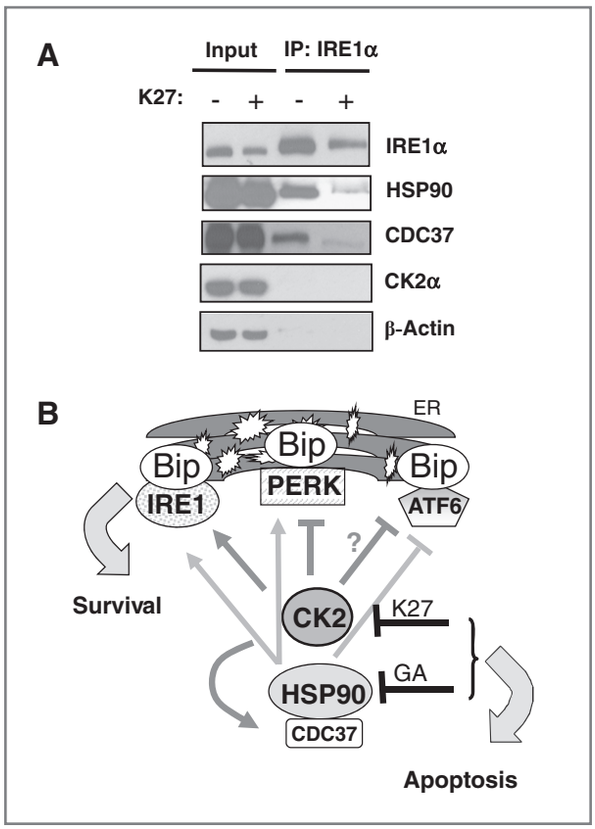

Figure 6. CK2α inhibition lowers the cellular levels of the complex formed by HSP90, CDC37, and IRE1α. A, co-immunoprecipitation (IP) of IRE1α protein, HSP90, and CDC37 was carried out in U-266 cells treated with K27 (5 μmol/L) for 3 hours. Co-immunoprecipitation using IRE1α antibody shows that less HSP90 and CDC37 were co-immunoprecipitated with IRE1α protein in sample treated with K27. Total cell extract (input) was used as loading control. CK2α did not co-immunoprecipitated with IRE1α. B, schematic model of CK2 and HSP90 cross-talk on IRE1α- and PERK-dependent UPR. Dark gray arrows refer to CK2, light gray arrows refer to HSP90.

response upregulated, protein synthesis and antibodies production are ensured (35). Under stressed conditions, CK2 inhibition potentiated thapsigargin-induced multiple myeloma cell apoptosis (Fig. 2). The increase of CK2 activity, IRE1α, BIP/GRP78, CHOP/GADD153, and phospho-Thr 981PERK protein levels, observed upon thapsigargin treatment, could represent an early attempt of the cells to cope with ER stress (35); indeed, thapsigargin-induced apoptosis was time-dependent, stronger at late time points, when it is likely that the prodeath pathways prevail over the compensatory mechanisms. CK2 inactivation together with thapsigargin interfered with the thapsigargin-induced compensatory UPR. Therefore, the cooperative anti–multiple myeloma cytotoxic effect of thapsigargin and CK2 inactivation could rely on a less effective early compensatory UPR and a shift toward an anticipated, stronger terminal UPR. The cooperation was also active in the presence of bone marrow stromal cells.

CK2 regulates the chaperoning activity of HSP90 through phosphorylation of the co-chaperone CDC37 at Ser13 (12). Clinical trials are currently testing HSP90 inhibitors in a number of tumors, including multiple myeloma (2, 10). HSP90 inhibitors induce multiple myeloma cell death also through the deregulation of the UPR (14, 15). Here, by showing that CK2 and HSP90 inactivation synergized in causing multiple myeloma cell death, as shown with different approaches in multiple myeloma cell lines, in models of multiple myeloma bone marrow microenvironment, in plasma cells from patients with multiple myeloma, and in the *in vivo* human myeloma mouse xenograft, we validated our hypothesis that CK2 could crosstalk with HSP90 in sustaining multiple myeloma cell survival (Fig. 3 and Supplementary Fig. S3). Remarkably, to our knowledge, the experiments with the mouse model are the first description of an *in vivo* anti-myeloma activity of CK2 inhibitors ever reported. Moreover, we provided original evidence that CK2 and HSP90 cooperate in maintaining IRE1α levels and activity, whereas they act in opposite ways on the PERK-dependent axis (Fig. 4). CK2 inactivation impaired the geldanamycin-induced expression of IRE1α–XBP1 targets, such as BIP/GRP78, triggered the transcription of the ATF6 target gene *EDEM*, and buffered down that of *CHOP/GADD153* (Fig. 5). Our data for the first time implicate CK2 in the transcription of ER stress/UPR-driven genes. The outcome of CK2 inhibition on CHOP/GADD153 levels deserves further investigation. *CHOP/GADD153* mRNA is upregulated by the IRE1α–XBP1, EIF2α–ATF4, and ATF6 branches (34). According to our results, these latter 2 cascades could be activated upon CK2 inhibition; therefore, *CHOP/GADD153* mRNA levels would be expected to increase. On the other hand, the strong impairment of IRE1α–XBP1, and perhaps of other transcription factors that stimulates CHOP/GADD153 expression, could account for the *CHOP/GADD153* mRNA decrease that we instead observed. However, reports have suggested a secondary role for CHOP in normal and malignant plasma cell survival (36, 37). It must be noted that the different effects obtained using K27 or CK2 silencing could be due, at least in part, to the different degree of CK2α protein activity reduction using the 2 approaches.

Mechanistically, CK2 inhibition resulted in a reduction of HSP90, CDC37, and IRE1α complexes in the cell, thus likely leading to accelerate IRE1α turnover (Fig. 6A). CK2 is known to associate with HSP90 and this interaction establishes a mutual regulation (38, 39).

Notably, the very recent finding that IRE1α could represent a therapeutic target for multiple myeloma provides a strong support for the importance of this signaling system in this blood tumor (40).

Figure 6B shows a model for CK2 and HSP90 cross-talk in the UPR. CK2 promotes cell survival controlling IRE1α levels and inhibiting PERK and EIF2α phosphorylation, thus sustaining a compensatory UPR. CDC37/HSP90 cooperates with CK2 stabilizing IRE1α but opposes CK2 on PERK activity. Our results on *EDEM1*—a main ATF6 target gene—mRNA expression suggest that CK2 could inhibit the ATF6-dependent response. The simultaneous inhibition of CK2 and induction of ER stress with thapsigargin or HSP90

Published OnlineFirst February 20, 2012; DOI:10.1158/1078-0432.CCR-11-1789

inhibitors produce a striking cytotoxic effect on multiple myeloma cells, most likely because of the abrogation of the compensatory IRE1α-mediated response.

CK2 inhibitors are currently being tested in phase I clinical trials in patients with multiple myeloma. The oral compound CX-4945 developed by Cylene (5) has displayed a considerable activity against a wide array of solid tumors and multiple myeloma (41) and affects the NF-κB, STAT3, and AKT signaling pathways (42), confirming the results that we previously obtained with other CK2 inhibitors and gene silencing (3). Thus, our and others' work imply that CK2 inhibition may represent a promising novel anti–multiple myeloma therapeutic approach. The data presented here reinforce this notion and provide novel clues on how CK2 might control multiple myeloma cell survival. Our results offer the groundwork to test in the clinical setting the combination of CK2 inactivation with drugs affecting the UPR, such as geldanamycin derivatives or other HSP90-targeting molecules or the currently widely used proteasome inhibitor bortezomib.

Disclosure of Potential Conflicts of Interest

No potential conflicts of interests were disclosed.

Authors' Contributions

Conception and design: S. Manni, M. Ruzzene, L.A. Pinna, F. Piazza
Development of methodology: S. Manni, F. Piazza
Acquisition of data (provided animals, acquired and managed patients, provided facilities, etc.): S. Manni, A. Brancalion, L.Q. Tubi, A. Colpo, L. Pavan, A. Cabrelle, E. Ave, F. Zaffino, G. Di Maira, M. Ruzzene, F. Adami, R. Zambello, M.R. Pitari, P. Tassone, C. Gurrieri, F. Piazza
Analysis and interpretation of data (e.g., statistical analysis, biostatistics, computational analysis): S. Manni, A. Brancalion, L.Q. Tubi, M. Ruzzene, C. Gurrieri, F. Piazza
Writing, review, and/or revision of the manuscript: S. Manni, M. Ruzzene, L.A. Pinna, G. Semenzato, F. Piazza
Administrative, technical, or material support (i.e., reporting or organizing data, constructing databases): L.Q. Tubi
Study supervision: G. Semenzato, F. Piazza

Acknowledgments

The authors thank the past and present members of the Hematological Malignancies Unit at the VIMM and patients for donating samples. They also thank Drs. Martina Pigazzi and Alessandra Beghin from the Department of Pediatrics "Salus Pueri", Laboratory of Hematology-Oncology, University of Padua, Padua Italy, for technical assistance in conducting the Gene Scan Fragment Analysis.

Grant Support

This work was supported by grants from the Ministry of University (FIRB - RBFR086EW9_001) to F. Piazza and from Associazione Italiana per la Ricerca sul Cancro (AIRC) to G. Semenzato.

The costs of publication of this article were defrayed in part by the payment of page charges. This article must therefore be hereby marked *advertisement* in accordance with 18 U.S.C. Section 1734 solely to indicate this fact.

Received July 11, 2011; revised January 20, 2012; accepted February 10, 2012; published OnlineFirst February 20, 2012.

References

1. Raab MS, Podar K, Breitkreutz I, Richardson PG, Anderson KC. Multiple myeloma. Lancet 2009;374:324–39.
2. Mitsiades CS, Hideshima T, Chauhan D, McMillin DW, Klippel S, Laubach JP, et al. Emerging treatments for multiple myeloma: beyond immunomodulatory drugs and bortezomib. Semin Hematol 2009;46:166–75.
3. Piazza FA, Ruzzene M, Gurrieri C, Montini B, Bonanni L, Chioetto G, et al. Multiple myeloma cell survival relies on high activity of protein kinase CK2. Blood 2006;108:1698–707.
4. Ruzzene M, Pinna LA. Addiction to protein kinase CK2: a common denominator of diverse cancer cells? Biochem Biophys Res Commun 2009;1804:499–504.
5. Ferguson AD, Sheth PR, Basso AD, Paliwal S, Gray K, Fischmann TO, et al. Structural basis of CX-4945 binding to human protein kinase CK2. FEBS Lett 2011;585:104–10.
6. Yahara I, Minami Y, Miyata Y. The 90-kDa stress protein, Hsp90, is a novel molecular chaperone. Ann N Y Acad Sci 1998;851:54–60.
7. Erlichman C. Tanespimycin: the opportunities and challenges of targeting heat shock protein 90. Expert Opin Investig Drugs 2009;18:861–8.
8. Mitsiades CS, Mitsiades NS, McMullan CJ, Poulaki V, Kung AL, Davies FE, et al. Antimyeloma activity of heat shock protein-90 inhibition. Blood 2006;107:1092–100.
9. Okawa Y, Hideshima T, Steed P, Vallet S, Hall S, Huang K, et al. SNX-2112, a selective Hsp90 inhibitor, potently inhibits tumor cell growth, angiogenesis, and osteoclastogenesis in multiple myeloma and other hematologic tumors by abrogating signaling via Akt and ERK. Blood 2009;113:846–55.
10. Richardson PG, Chanan-Khan AA, Alsina M, Albitar M, Berman D, Messina M, et al. Tanespimycin monotherapy in relapsed multiple myeloma: results of a phase 1 dose-escalation study. Br J Haematol 2010;150:438–45.
11. Brown MA, Zhu L, Schmidt C, Tucker PW. Hsp90–from signal transduction to cell transformation. Biochem Biophys Res Commun 2007;363:241–6.
12. Miyata Y, Nishida E. CK2 controls multiple protein kinases by phosphorylating a kinase-targeting molecular chaperone, Cdc37. Mol Cell Biol 2004;24:4065–74.
13. Miyata Y. Protein kinase CK2 in health and disease: CK2: the kinase controlling the Hsp90 chaperone machinery. Cell Mol Life Sci 2009;66:1840–9.
14. Davenport EL, Moore HE, Dunlop AS, Sharp SY, Workman P, Morgan GJ, et al. Heat shock protein inhibition is associated with activation of the unfolded protein response pathway in myeloma plasma cells. Blood 2007;110:2641–9.
15. Patterson J, Palombella VJ, Fritz C, Normant E. IPI-504, a novel and soluble HSP-90 inhibitor, blocks the unfolded protein response in multiple myeloma cells. Cancer Chemother Pharmacol 2008;61:923–32.
16. Mori K. Signalling pathways in the unfolded protein response: development from yeast to mammals. J Biochem 2009;146:743–50.
17. Rasheva VI, Domingos PM. Cellular responses to endoplasmic reticulum stress and apoptosis. Apoptosis 2009;14:996–1007.
18. Ron D, Walter P. Signal integration in the endoplasmic reticulum unfolded protein response. Nat Rev Mol Cell Biol 2007;8:519–29.
19. Ni M, Lee AS. ER chaperones in mammalian development and human diseases. FEBS Lett 2007;581:3641–51.
20. Iwakoshi NN, Lee AH, Vallabhajosyula P, Otipoby KL, Rajewsky K, Glimcher LH. Plasma cell differentiation and the unfolded protein response intersect at the transcription factor XBP-1. Nat Immunol 2003;4:321–9.
21. Carrasco DR, Sukhdeo K, Protopopova M, Sinha R, Enos M, Carrasco DE, et al. The differentiation and stress response factor XBP-1 drives multiple myeloma pathogenesis. Cancer Cell 2007;11:349–60.
22. Hessenauer A, Schneider CC, Gotz C, Montenarh M. CK2 inhibition induces apoptosis via the ER stress response. Cell Signal 2011;23:145–51.
23. Piazza F, Manni S, Tubi LQ, Montini B, Pavan L, Colpo A, et al. Glycogen Synthase Kinase-3 regulates multiple myeloma cell growth and bortezomib-induced cell death. BMC Cancer 2010;10:526.

Published OnlineFirst February 20, 2012; DOI:10.1158/1078-0432.CCR-11-1789

24. Sotiropoulou PA, Perez SA, Salagianni M, Baxevanis CN, Papamichail M. Characterization of the optimal culture conditions for clinical scale production of human mesenchymal stem cells. Stem Cells 2006;24:462–71.
25. Burger R, Guenther A, Bakker F, Schmalzing M, Bernand S, Baum W, et al. Gp130 and ras mediated signaling in human plasma cell line INA-6: a cytokine-regulated tumor model for plasmacytoma. Hematol J 2001;2:42–53.
26. Ruzzene M, Penzo D, Pinna LA. Protein kinase CK2 inhibitor 4,5,6,7-tetrabromobenzotriazole (TBB) induces apoptosis and caspase-dependent degradation of haematopoietic lineage cell-specific protein 1 (HS1) in Jurkat cells. Biochem J 2002;364:41–7.
27. Kang HS, Welch WJ. Characterization and purification of the 94-kDa glucose-regulated protein. J Biol Chem 1991;266:5643–9.
28. Iwakoshi NN, Lee AH, Glimcher LH. The X-box binding protein-1 transcription factor is required for plasma cell differentiation and the unfolded protein response. Immunol Rev 2003;194:29–38.
29. Sarno S, Papinutto E, Franchin C, Bain J, Elliott M, Meggio F, et al. ATP site-directed inhibitors of protein kinase CK2: an update. Curr Top Med Chem 2011;11:1340–51.
30. Marcu MG, Doyle M, Bertolotti A, Ron D, Hendershot L, Neckers L. Heat shock protein 90 modulates the unfolded protein response by stabilizing IRE1alpha. Mol Cell Biol 2002;22:8506–13.
31. Faust M, Jung M, Gunther J, Zimmermann R, Montenarh M. Localization of individual subunits of protein kinase CK2 to the endoplasmic reticulum and to the Golgi apparatus. Mol Cell Biochem 2001;227:73–80.
32. Yamane K, Kinsella TJ. CK2 inhibits apoptosis and changes its cellular localization following ionizing radiation. Cancer Res 2005;65:4362–7.
33. Gotz C, Muller A, Montenarh M, Zimmermann R, Dudek J. The ER-membrane-resident Hsp40 ERj1 is a novel substrate for protein kinase CK2. Biochem Biophys Res Commun 2009;388:637–42.
34. Kim I, Xu W, Reed JC. Cell death and endoplasmic reticulum stress: disease relevance and therapeutic opportunities. Nat Rev Drug Discov 2008;7:1013–30.
35. Rutkowski DT, Hegde RS. Regulation of basal cellular physiology by the homeostatic unfolded protein response. J Cell Biol 2010;189:783–94.
36. Nerini-Molteni S, Ferrarini M, Cozza S, Caligaris-Cappio F, Sitia R. Redox homeostasis modulates the sensitivity of myeloma cells to bortezomib. Br J Haematol 2008;141:494–503.
37. Masciarelli S, Fra AM, Pengo N, Bertolotti M, Cenci S, Fagioli C, et al. CHOP-independent apoptosis and pathway-selective induction of the UPR in developing plasma cells. Mol Immunol 2010;47:1356–65.
38. Miyata Y, Yahara I. The 90-kDa heat shock protein, HSP90, binds and protects casein kinase II from self-aggregation and enhances its kinase activity. J Biol Chem 1992;267:7042–7.
39. Miyata Y, Yahara I. Interaction between casein kinase II and the 90-kDa stress protein, HSP90. Biochemistry 1995;34:8123–9.
40. Papandreou I, Denko NC, Olson M, Van Melckebeke H, Lust S, Tam A, et al. Identification of an Ire1alpha endonuclease specific inhibitor with cytotoxic activity against human multiple myeloma. Blood 2010;117:1311–4.
41. Padgett CS, Lim JKC, Marschke RF, Northfelt DW, Andreopoulou E, Von Hoff DD, et al. Clinical pharmacokinetics and pharmacodynamics of CX-4945, a novel inhibitor of protein kinase CK2: interim report from the phase 1 clinical trial. Eur J Cancer Suppl 2010;8:131–2.
42. Ho C, Rice R, Drygin D, Bliesath J, Streiner N, Siddiqui-Jain A, et al. CX-4945, a selective and orally bioavailable inhibitor of protein kinase CK2 inhibits PI3K/Akt, JAK-STAT and NF-kB signaling and induces apoptosis in multiple myeloma cells. Blood (ASH annual meeting abstracts) 2010;116:787.